Taran, M. N., Koch-Müller, M., Feenstra, A. (2009): Optical spectroscopic study of tetrahedrally coordinated Co2+ in natural spinel and staurolite at different temperatures and pressures. - American Mineralogist, 94, 11-12, 1647-1652

DOI: 10.2138/am.2009.3247

Optical spectroscopic study of tetrahedrally coordinated Co^{2+} in natural spinel and staurolite at different temperatures and pressures

Michail N. Taran[1], Monika Koch-Müller[2] and Anne Feenstra[3]

[1]Institute of Geochemistry, Mineralogy and Ore Formation, National Academy of Science of Ukraine, Palladin Ave., 34, 03680 Kyiv-142, Ukraine, E-mail: taran@igmr.relc.com

[2] Deutsches GeoForschungsZentrum, Sektion 3.3, Telegrafenberg, 14473 Potsdam, Germany, e-mail: mkoch@gfz-potsdam.de

[3]deceased on April 9, 2007

Abstract

Optical absorption spectra of natural Co-bearing spinel and staurolite were studied at different temperatures and pressures. In both minerals two broad intense structured bands in the range 5500 - 8000 cm^{-1} and 15000 - 19000 cm^{-1}, caused by electronic spin-allowed transitions $^4A_2 \rightarrow {}^4T_1(^4F)$ and $^4A_2 \rightarrow {}^4T_1(^4P)$ of $^{IV}Co^{2+}$ are the predominant absorption features. In addition, in both cases broad bands, derived from spin-allowed electronic transitions $^4E \rightarrow {}^4T_2$ of $^{IV}Fe^{2+}$, appear in the near infrared range partly overlapping the bands caused by $^{IV}Co^{2+}$. In staurolite the NIR range of the spectra are complicated by intense sharp lines of OH-vibrations at around 3400 cm^{-1}.

In spinel with a regular tetrahedral site the splitting of the spin-allowed bands I and II of $^{IV}Co^{2+}$ is assumed to be caused by spin-orbit and vibronic coupling. In staurolite the splitting is stronger due to the additional low symmetry crystal field effect of $^{IV}Co^{2+}$. It is found that the effect of temperature and pressure on the behavior the $^4A_2 \rightarrow {}^4T_1(^4P)$ bands of $^{IV}Co^{2+}$ in the two minerals are rather similar in contrast to our findings for the spin-allowed bands of $^{IV}Fe^{2+}$ in spinel and staurolite. This is interpreted as a manifestation of a dynamic Jahn-Teller effect of $^{IV}Fe^{2+}$ and lack of it in case of $^{IV}Co^{2+}$.

Key words: spinel, staurolite, tetrahedral coordination, Co^{2+}, optical absorption spectra, temperature and pressure effects

Introduction

Temperature and pressure effects on spin-allowed *dd*-bands originating from $^5E \rightarrow {}^5T_2$ transition of tetrahedral Fe^{2+} in natural spinel were found to be rather different from staurolite (Taran and Koch-Müller, 2009). This was attributed to a dynamic Jahn-Teller effect, intrinsic to electronic centers with two-fold degenerated ground state *E*, in spinel (Taran and Langer, 2001, Taran et al., 2005) and suppressed by a static crystal field distortion in staurolite (Taran and Koch-Müller, 2009).

Co^{2+}, which also occupies tetrahedral sites in both spinel and staurolite structures (e.g. Burns, 1993), is not expected to show a Jahn-Teller effect since the ground electronic level of $^{IV}Co^{2+}$ is a non-degenerated $^4A_2$-state. Therefore, the effect of pressure or temperature on the behavior of the absorption crystal field bands of $^{IV}Co^{2+}$ of the two minerals should be quite similar. In this paper the results of a comparative optical spectroscopic study of natural Co^{2+}-bearing spinel and staurolite at different pressures and temperatures are presented.

Experimental details

Samples and chemical composition

Staurolite and spinel for the present study were collected from diaspore-bearing metabauxite lens on the eastern coast of the island of Samos (the eastern part of the Aegean Sea, Greece) near Mikri Lakka (the sample no. Sa9a in Feenstra et al., 2003). The rock consists of silicate- and oxide-rich domains or layers in a matrix of calcite with a minor amount of muscovite and paragonite. After crashing to a coarse powder and cleaning from calcite by dissolution in concentrated HCl, several perfectly transparent and homogeneously colored dark-blue octahedral crystals of gahnite spinel of "the second generation" (Feenstra et

al., 2003) of ~0.2 mm in diameter were selected for an optical absorption spectroscopy study. The electron microprobe analysis (EMPA) is similar to that of sample no. Sa9a (a) in Tab. 3 by Feenstra et al. (2003): $(Fe_{0.078}Mg_{0.011}Mn_{0.03}Zn_{0.865}Ni_{0.006}Co_{0.019})_{0.982}$ $(Si_{0.001}Ti_{0.002}Al_{2.003}Cr_{0.006})_{2.011}O_4$. Thin plates of thickness ca. 0.05 mm were prepared by polishing the crystals on two opposite sides with diamond pastes. They were used for optical absorption spectroscopy at ambient conditions, as well as at higher temperatures (up to 300 °C) and pressures (up to 12 GPa).

Two sections of Co-bearing staurolite, **ac** (010) and **ab** (001)**,** prepared from fragments of a single crystal polished on both sides as thin plates of ~0.08 mm thickness were used for measuring polarized optical absorption spectra at ambient conditions and at different temperatures. At unpolarized transmitting illumination they are homogeneously colored in blue and violet-blue color, respectively. Unpolarized high-pressure spectra were measured on a thinner plate (~0.05 mm) of a random orientation prepared from a tiny fragment of this same crystal.

Chemical compositions (Cameca SX100 electron microprobe) of the two plates in **ac** (010)- and **ab** (001)-orientation were measured close to the spots where the spectra were taken. Standards for the EMPA included the following synthetic and natural minerals and metals: garnets (Fe, Mn, Si, Al); ilmenites (Fe, Mn, Ti); rutile (Ti); wollastonite (Ca, Si); spinel (Mg, Al); corundum (Al); periclase (Mg); gahnite (Zn, Al); sphalerite (Zn); escolaite (Cr); NiO (Ni); metallic V, Zn, Ni and Co. The average crystal chemical formula for both sections, (010) and (001), calculated on the basis of 46 oxygens are presented in Tab. 1. For more clearness we display it also here: $(Fe^{2+}_{0.831}Mg_{0.089}Mn_{0.034}Zn_{1.648}Ni_{0.203}Co_{0.175}Li_{0.740})_{3.720}$ $(Ti_{0.037}Al_{17.591}Cr_{0.008})_{17.736}(Si_{8.087}Al_{0.028})_{8.089}O_{46}$ – the **ac**-section, (010); $(Fe^{2+}_{0.587}Mg_{0.117}Mn_{0.032}Zn_{1.593}Ni_{0.069}Co_{0.109}Li_{0.745})_{3.252}(Ti_{0.012}Al_{17.749}Cr_{0.029})_{17.791}Si_{8.214}O_{46}$ – the **ab**-section, (001).

The Li-content was determined by secondary ion mass spectrometry (SIMS). Because Fe > Co, Mg (Tab. 1) in our sample, the mineral is referred to as Co-bearing staurolite and not lusakite. For lusakite Co, Mg should be higher than Fe (e.g. Bringhurst and Greefen 1986).

Spectroscopic measurements

Spectra in the range ca. 35000 - 8000 cm^{-1} were measured with a home-made microspectrophotometer described elsewhere (e.g. Taran et al., 2008). Spectra in the range 8000 -3000 cm^{-1} were measured on a Bruker IFS 66v FTIR spectrometer equipped with a Hyperion microscope. All conditions of spectroscopic measurements were taken close to those described by e.g. Taran et al. (2005). High-temperature spectra of both, spinel and staurolite, and high-pressure spectra of spinel were scanned in the range ~29000-10000 cm^{-1}.

Results

Ambient conditions

A spectrum of Co-bearing spinel, measured at ambient conditions in the range 35000-6000 cm^{-1}, is shown in Fig. 1. Energies of the main bands of $^{IV}Co^{2+}$ observed are compiled in Tab. 2. Apart from a high-energy absorption edge in the UV range (~32000 cm^{-1}) and a weak peak *g*, there are two dominating broad absorptions in the near infrared and visible, I and II, both split to three main components designated as *a*, *b*, *c* (band I) and *d*, *e*, *f* (band II). In addition, the bands *b*, *c*, *e* and *f* are all obviously a combination of at least two sub-components. The broad split band at around ~5000 cm^{-1} is caused by $^{IV}Fe^{2+}$ (see Discussion). The band II in the visible range absorbs yellow-orange-red light thus causing blue coloration of Co-bearing spinels.

Polarized spectra of Co-bearing staurolite are shown in Fig. 2; energies of the main bands are given in Tab. 2. As seen from Fig. 2, besides a strongly **E**||**c**-polarized high-energy edge there are two distinct bands, one in near infrared range (band I) and one in the visible

range (band II) which both are obviously due to $^{IV}Co^{2+}$. The two bands are split to three main strongly polarized components, *a*, *b*, *c* and *f*, *g*, *h*, respectively. The low-energy wing of the band I is complicated by strong lines of the OH vibrations. Besides, in all three polarizations there are two weak features, *d* and *e*, superimposed on the high-energy wing of the band I.

Due to the strong polarization dependence of the split components of band II the sample displays a distinct pleochroism, sky-blue (**E**||**b**), blue (**E**||**a**) and violet-blue (**E**||**c**), quite in accordance with e.g. Skerl et al. (1934**)**.

High-temperature spectra

Increasing temperature produces similar effects on the behavior of band II in the spectra of both spinel and staurolite. As seen from Figs. 3 and 4 the linear intensity of the band decreases with increasing temperature and the band and its split components become broader such that the integral intensity remains nearly constant. Although the barycenter of the band in spinel nearly shows no change in energy with increasing temperature, the two outer bands *d* and *f* evidently shift to opposite directions. The central band *e*, which split at room temperature to at least two components, shifts with increasing temperature to higher energies and becomes more symmetric and narrower.

In staurolite the maxima of the *g*- and *h*-band also nearly show no change in energy with increasing temperature, whereas the band *f* displays a distinct shift to lower energies, causing a slight shift of the band's II barycenter to lower energies (Fig. 4).

High-pressure spectra

Under pressure all Co^{2+}-bands in spinel and staurolite shift to higher energies without any significant change in the integral intensity (Figs. 5, 6). In the spinel spectra (Fig. 5), one of the band's II split components, namely band *d*, significantly decreases in intensity, whereas another one, band *e*, noticeably increases with increasing pressure thus leaving the integral

intensity nearly constant. The splitting of the bands *e* and *f* noticeably increases under pressure.

In an unpolarized spectrum of the staurolite crystal (Fig. 6), the structure of the NIR band I is, obviously, a superposition of three bands *a* to *c* (see **E**||**a**- and **E**||**c**-polarized spectra in Fig. 2), the *c* band being most distinct. Besides, absorption lines of the pressure transmitting medium, vaseline, appear in the range 3800-4500 cm^{-1} strongly interfering the observation of band I. There is also a series of very strong absorption lines around 3500 cm^{-1}, caused by OH-vibrations. The two weak features, *d* and *e*, superimposed on the high-energy wing of the band I, become more distinct evidently increasing in intensity and both shift to higher energies from ca. 8250 and 7360 cm^{-1}, respectively, at atmospheric pressure to ~8880 and 8020 cm^{-1} at 12 GPa. The band II in the visible range consists of three split components designated above as *f*, *g* and *h* (cf. Fig. 2).

With increasing pressure the overall splittings of two bands I and II obviously increase. Thus, at ~10.2 GPa the pressure-induced high-energy shifts of the two outer components of the band II, *f* and *h*, are different, ~300 cm^{-1} versus ~430 cm^{-1}, respectively, evidencing the increased splitting. Besides, the bands *c* and *g*, components of, respectively, band I and II, split additionally into two distinct sub-components.

Discussion

A polarized spectrum of natural Co-staurolite, lusakite, from Zambia was first published by Burns (1993). He assigned the observed absorption bands to tetrahedral Co^{2+} pointing out a certain similarity with a spectrum of, probably, synthetic Co-doped spinel. As far as we are aware, spectra of natural Co^{2+}-bearing spinel were not yet published.

In spinel Co^{2+} occupies a regular tetrahedron of T_d point symmetry (e.g., Yamanaka and Takéuchi, 1983) with four equal M-O bond lengths varying from ~1.911 Å in $MgAl_2O_4$ (Peterson et al. 1991) to ~1.968 Å in $ZnAl_2O_4$ (Levy et al. 2001). In staurolite the Fe-

tetrahedron, accommodating Co^{2+}, consists of two oxygens and two hydroxyls: 2 × (Fe-O) =1.971 Å, 2 × (Fe-OH) = 2.035 Å. The local symmetry is close to C_{2v} (Koch-Müller, 1997).

Considered as the three-hole case, tetrahedral Co^{2+} has the same energy level scheme as a Cr^{3+} ion in octahedral symmetry. The spin-allowed absorption bands arise from the two quartet terms, ^4F and ^4P, of the free ion. A series of spin-forbidden bands may appear due to electronic transitions to the exited states derived from ^2G, ^2P, ^2H, ^2D or ^2F terms.

From the theory and according to the Tanabe-Sugano diagram for tetrahedral Co^{2+} (e.g. Alonso and Alcalá, 1977) three spin-allowed electronic transitions with increasing transition energies are expected: $^4A_2 \rightarrow {}^4T_2(^4F)$, $^4A_2 \rightarrow {}^4T_1(^4F)$ and $^4A_2 \rightarrow {}^4T_1(^4P)$. Assuming, very reasonably, that in the two minerals, spinel and staurolite, Co^{2+} does occupy the tetrahedral sites of their structures (Feenstra et al., 2003; Bringhurst and Greefen,1986; Phillips and Griffen, 1986; Burns, 1993) and taking into account that in the tetrahedral coordination the crystal field strength *Dq* is considerably reduced so that the two first excited level $^4T_2(^4F)$ and $^4T_1(^4F)$ of $^{IV}Co^{2+}$ should be observed in the infrared, in accordance with the Tanabe-Sugano diagram for electronic d^7-configuration in tetrahedral or cubic crystal fields (e.g. Alonso and Alcalá, 1977) the two main absorption bands I and II in the spectra in Figs. 1 and 4 should be assigned to the spin-allowed electronic transitions $^4A_2 \rightarrow {}^4T_1(^4F)$ and $^4A_2 \rightarrow {}^4T_1(^4P)$, respectively, of $^{IV}Co^{2+}$. The third, the lowest energy spin-allowed transition of Co^{2+}, $^4A_2 \rightarrow {}^4T_2(^4F)$, occurs, according to Ferguson et al. (1969) for synthetic Co^{2+}-bearing $ZnAl_2O_4$ spinel, as a very weak structured band at ca. 4500 cm^{-1}. Similarly, in a spectrum of synthetic Co^{2+}-bearing $MgAl_2O_4$ Dereń et al. (1994) found a weak band centered around 4200 cm^{-1} which was also attributed to $^4A_2 \rightarrow {}^4T_2(^4F)$ transition of $^{IV}Co^{2+}$. From these we can conclude that in our natural spinel (Fig. 1) $^4A_2 \rightarrow {}^4T_2(^4F)$ band should be somewhere in the range 4200 to 4500 cm^{-1}. However, it can not be seen as it is very weak (2-3% of the intensity of band I,

$^4A_2 \rightarrow {}^4T_1(^4\mathrm{F})$, see Ferguson et al. (1969))[1] and overlapped by much more intense bands of the spin-allowed $^5E \rightarrow {}^5T_2$ transition of $^{IV}Fe^{2+}$ seen as a broad doublet with maxima around 4900 cm^{-1} and 3700 cm^{-1}, similar to the descriptions by Rossman and Taran (2001), Skogby and Hålenius (2003) and Taran et al. (2005). This feature is designated in the Figure as $^{IV}Fe^{2+}$. Note also that the above interpretation of $^{IV}Co^{2+}$ bands fairly agrees with those of a number of synthetic Co^{2+}-bearing spinels of various compositions (Hochu and Lenglet, 1998), silicate glasses (Keppler, 1992), $CoCl_2$ in different solvents (Antipova-Karataeva and Rzhevskaya, 1974) and various Co-bearing fused solutions (Gruen and McBeth, 1963), all containing Co^{2+} in tetrahedral coordination.

From energies ν_1 and ν_2 of the $^4A_2 \rightarrow {}^4T_2(^4F)$ and $^4A_2 \rightarrow {}^4T_1(^4F)$ transitions, respectively, the value of the Racah parameter B may be evaluated using the expression $B = \frac{1}{3}\frac{(2\nu_1 - \nu_2)(\nu_2 - \nu_1)}{(9\nu_1 - 5\nu_2)}$, i.e. the same as for Cr^{3+} (e.g. Burns, 1993). Assuming that ν_1 = 4200 cm^{-1} (see above) and ν_2 = 7150 cm^{-1}, i.e. ca. the mean value of the energies of the *a*, *b*, and *c*-bands of spinel in Table 2, it gives $B \approx 600$ cm^{-1}, which is significantly reduced compared to 1030 cm^{-1} for the free Co^{2+}, (e.g. Bersuker 1996). This evidences increased covalency of the Co-O bonds in the CoO_4-tetrahedra. It should also be noted that the obtained value of the *B*-parameter is appreciably smaller than those obtained by Hochu and Lenglet (1998) from diffuse reflectance spectra of a series of Co-bearing spinels. However, these authors did not specify in what exactly way the B-values have been calculated: evidently, not from energies of the $^4A_2 \rightarrow {}^4T_2(^4F)$ and $^4A_2 \rightarrow {}^4T_1(^4F)$ transitions as in our case, since no data on the former band were obtained.

[1] According to Ferguson (1963) and Ferguson et al. (1969), in the tetrahedral symmetry the $^4A_2 \rightarrow {}^4T_2(^4F)$ transition of Co^{2+} is forbidden for electronic dipole absorption but is allowed for magnetic dipole radiation. Due to the effect of spin-orbit coupling the $^4T_2$-state can be mixed with the two $^4T_1$ states and the transition can be partly allowed as electronic dipole one. Another interpretation of the weak intensity of the $^4A_2 \rightarrow {}^4T_2(^4F)$ band is its two-electron jump nature, $t_2^3e^4 \rightarrow t_2^5e^2$ (e.g. Marfunin, 1979), which makes the probability of the transition very low.

The pronounced structure of the Co^{2+} bands I and II (Fig. 1) results from spin-orbit and/or vibronic interactions, typical for electronic transitions of Co^{2+} (e.g., Marfunin, 1979). Additionally, in the range of band II a number of spin-forbidden bands may appear caused by $^4A_2(^4F) \rightarrow {}^2E(^2G)$, $^4A_2(^4F) \rightarrow {}^2A_1(^2G)$ and $^4A_2(^4F) \rightarrow {}^2T_1(^2G)$, transitions of $^{IV}Co^{2+}$ (Ferguson et al., 1969, Alonso and Alcalá, 1977) which make an assignment very difficult. At least, the weak *g*-band is very likely one of these three transitions, most probably, the latest one (cf. Ferguson et al., 1969, Dereń et al., 1994).

As seen from Fig. 2, in staurolite the splitting of the two bands, I and II, is appreciably stronger than in spinel due to the effect of the low symmetry crystal field of the tetrahedral Fe-site, accommodating Co^{2+}, which is close to C_{2v} (Koch-Müller, 1997) and causes an additional splitting of the exited electronic levels of $^{IV}Co^{2+}$. Besides that, the low energy band I is obviously intensified and complicated by a contribution of tetrahedral ferrous ions: the broad split spin-allowed *dd*-bands caused by electronic $^5E \rightarrow {}^5T_2$ transition of $^{IV}Fe^{2+}$, appear in this same spectral range (Rossman and Taran, 2001; Taran and Koch-Müller, 2009). Particularly, the broad band at ~4000 cm^{-1} in **E**||**c**-polarization, marked as $^{IV}Fe^{2+}$ in Fig. 2, closely corresponds to **E**||**c**-polarized band III in the spectrum of Fe-rich staurolite (Taran and Koch-Müller, 2009). Note in this respect that the iron concentration in the staurolite and spinel samples studied is even higher than that of cobalt (see the Samples and chemical composition section and also Tab. 3 in Feenstra et al. (2003) and Tab. 1 in this paper). Nevertheless, probably, due to difference in the oscillator strength of the electronic *dd*-transitions of Co^{2+} and Fe^{2+} the absorption bands caused by Co^{2+} predominate in the spectra in Figs. 1, 2.

Apart from cobalt and iron, nickel - another transition metal - is also incorporated in spinel and staurolite of this study in concentrations commensurable or even exceeding that of cobalt (the Samples and chemical composition section and Tab. 1). However, due to the

strong preference of Ni^{2+} for octahedral sites (e.g. Taran et al., 2008) its spin-allowed bands, forbidden in octahedral crystal field by symmetry selection rules (e.g., Burns 1993), should be much weaker than those of tetrahedral, non-centrosymmetric Co^{2+}. For instance, the oscillator strength of the spin-allowed ${}^4T_{1g} \rightarrow {}^4T_{2g}$ transition of octahedral Ni^{2+} in CdI_2 is evaluated as $5.7 \cdot 10^{-5}$ (Kuindersma et al., 1981), whereas in spectra of Co-doped KCl, where Co^{2+} occupies the tetrahedral sites, the near infrared (5700 cm^{-1}) and visible (15000 cm^{-1}) bands caused by ${}^4A_2 \rightarrow {}^4T_1({}^4F)$ and ${}^4A_2 \rightarrow {}^4T_1({}^4P)$ transitions of ${}^{IV}Co^{2+}$, are much more intense, having, respectively, oscillator strength values $5 \cdot 10^{-4}$ and $30 \cdot 10^{-4}$ (Nasu, 1975). In synthetic $MgAl_2O_4$ spinel such values are estimated to be even higher, $0.2 \cdot 10^{-3}$ and $0.14 \cdot 10^{-2}$, respectively (Dereń et al., 1994). Thus, in spite of the relatively high nickel contents no crystal field bands of Ni^{2+} are readily observed in the spinel spectra of the two samples, spinel and staurolite (Fig. 1, 2). On the other hand, the origin of the two distinct absorption features, *d* and *e*, in the staurolite spectrum (Fig. 2) is not quite clear. Judging from the Tanabe-Sugano diagram for d^7-configuration in tetrahedral coordination (e.g. Alonso and Alcalá, 1977) they are unlikely caused by ${}^{IV}Co^{2+}$. In spectra of synthetic $NaScSi_2O_6 - CaNiSi_2O_6$ pyroxenes ${}^{VI}Ni^{2+}$(M1) gives rise a broad band at around 7800 cm^{-1} caused by the electronic spin-allowed transition ${}^3A_{2g} \rightarrow {}^3T_{2g}$ (Taran et al., 2008). The bands *d* and *e* in the spectrum of staurolite (Fig. 2) may be due to such transition of Ni^{2+} in the octahedral Al-sites of the structure, although in the crystal chemical formula of the staurolite studied, Ni^{2+}, as well as all other divalent cations, is formally posed in the tetrahedral Fe-site (see the Experimental section). The distinct pressure-induced shifts of the *d*- and *e*-bands to higher energies (Fig. 6) is rather consistent with such an interpretation as a similar shift of the ${}^3A_{2g} \rightarrow {}^3T_{2g}$ band of ${}^{VI}Ni^{2+}$ was observed also in the high-pressure spectra of $NaScSi_2O_6 - CaNiSi_2O_6$ pyroxenes (Taran et al., 2008). On the other hand, we should note that no bands caused by two another spin-allowed transitions of ${}^{VI}Ni^2$,

$^3A_{2g} \rightarrow {}^3T_{1g}$ and $^3A_{2g} \rightarrow {}^3T_{1g}(^3P)$, which in the orthopyroxene spectra appear at ~13000 and 24100 cm^{-1}, respectively, are seen in Fig. 6.

The temperature dependencies of the band II in the two samples, spinel and staurolite, are rather similar (see Result section and also Figs. 3, 4): there are some shifts to lower energies and redistribution of intensity between split components of band II, but the integral intensity of band II remains nearly constant. The split may be caused by spin-orbit and vibronic effects on the electronic transition $^4A_2 \rightarrow {}^4T_1(^4P)$ of $^{IV}Co^{2+}$ and also, very probably, by spin-forbidden transitions of $^{IV}Co^{2+}$ (see above). On the whole such a temperature dependence differs from findings for synthetic Co-bearing garnet, where the complex split band caused by $^4A_{2g} \rightarrow {}^4T_{1g}(^4P)$ transitions of $^{VIII}Co^{2+}$, significantly decreases in intensity with increasing temperature (Taran et al., 2002). This evidences that coordination and symmetry play an important role in the intensity gaining mechanism of absorption bands of Co^{2+}: the relatively weak temperature dependence of the transitions in spinel and staurolite is in accordance with the non-centrosymmetric character of Co^{2+} in their structures, however the strong weakening in garnet with Co^{2+} in eight-coordinated site, regarded as a strongly distorted cube, does not have such a simple explanation. It is worth mentioning that in difference to garnets, in CaF_2 with Co^{2+} in a regular cubic coordination, the intensity of the $^4A_{2g} \rightarrow {}^4T_{1g}(^4P)$ band increases with temperature (Alonso and Alcalá, 1977) just as expected for a centrosymmetric case.

Pressure induces effects on the behavior of the $^{IV}Co^{2+}$-bands in spinel and staurolite, which are in many respects opposite to the influence of temperature (Result section and also Figs. 5, 6). The high-energy shifts of the bands are due to compression of the structure and, thus, shortening of Co-O and Co-OH bonds under pressure. The weakening and almost disappearing of the split component *d* of the band II in the spinel spectra (Fig. 5) reminds closely of observations for the *e*-band in spectra of synthetic cobalt aluminum silicate garnets (Taran et al. 2002). It was assumed that in the garnets such pressure-induced behavior is due to the fact that in

difference to other split components derived from spin-allowed $^4A_{2g} \rightarrow {}^4T_{1g}(^4P)$ transition of $^{VIII}Co^{2+}$, the *e*-band is caused by a spin-forbidden transition $^4A_{2g} \rightarrow {}^2T_{1g}(^2G)$, although a reason for such pressure-induced decrease in intensity still is not clear. It seems now that a rather strong dependence of the intensity of some electronic transitions on pressure, either positive or negative, is rather typical for Co^{2+} in various coordinations.

Another aspect of the pressure effect on spectra of $^{IV}Co^{2+}$ in both spinel and staurolite is the distinct increase of the splitting of some components of band I and II. This is especially well seen on the *e*- and *f*-band in the spinel spectrum (Fig. 5) and the band *c* and *g* in staurolite (Fig. 6). This effect is quite different from what is expected: usually in high-pressure spectra of, for instance, Fe^{2+}- or Mn^{3+}-bearing minerals where Fe^{2+} and Mn^{3+} occupy distorted octahedral sites (e.g. Abu-Eid, 1976) the band splitting decreases due to a decrease of the distortion of the coordination polyhedra at hydrostatic compression. It seems certain that in case of Co^{2+}, where splitting of the spin-allowed bands is mainly due to spin-orbit coupling, hydrostatic compression of the structure causes either a decrease or an increase of the splitting and a significant redistribution of intensity between the split components. Such pressure-induced effects are not yet understood and not yet experimentally studied in any detail.

Summarizing, it is essential to notify that for $^{IV}Co^{2+}$ in spinel and staurolite the temperature and pressure effects on the optical absorption spectra are rather similar. This is different to our observation for $^{IV}Fe^{2+}$: as found by Taran and Langer (2001), Taran et al. (2005) and Taran and Koch-Müller (2009), the temperature and pressure effects on the absorption bands originating from electronic spin-allowed transitions $^5E \rightarrow {}^5T_2$ of $^{IV}Fe^{2+}$ in spinel and staurolite are significantly different. We attribute this to a manifestation of a dynamic Jahn-Teller effect on $^{IV}Fe^{2+}$ - intrinsic to spinel with regular tetrahedra of the structure, but suppressed by the low-symmetry crystal field of $^{IV}Fe^{2+}$ (ca. C_{2v}) in staurolite. As $^{IV}Co^{2+}$ has no Jahn-Teller effect, because its electronic ground state is $^4A_2$-singlet (e.g. Bersuker, 1996), there is no significant

difference in the temperature and pressure behavior of the spin-allowed bands of $^{IV}Co^{2+}$ in spinel and staurolite.

Acknowledgement

We are thankful to the German Science Foundation, Bonn-Bad Gobesberg that generously supported this work through traveling grant no KO1260/10 for MNT. The official reviewer, Manfred Wildner (Vienna) gave many comments, suggestions and corrections which allowed significant improving of the paper.

References

Abu-Eid, R.M. (1976) Absorption spectra of transition metal-bearing minerals at high pressures. In R.G.J. Strens, Ed., The Physics and Chemistry of Minerals and Rocks, p. 641–675. Wiley, New York.

Alonso, P.J. and Alcalá, R. (1977) On the optical absorption spectrum of Co^{2+} in CaF_2. Physica status solidi (b), 81, 333 – 339.

Antipova-Karataeva, I.I. and Rzhevskaya, N.N. (1974) A spectrophotometric study of cobalt (II) chloride in alcohol solutions. Theoretical and Experimental Chemistry, 8, 101-104.

Bringhurst, K.N. and Griffen, D.T. (1986) Staurolite-lusakite series. II. Crystal structure and optical properties of a cobaltoan staurolite. American Mineralogist, 71, 1466-1472.

Burns, R.G. (1993) Mineralogical applications of crystal field theory. 2nd ed. Cambridge University Press, Cambridge

Bersuker, I.B. (1996) Electronic Structure and Properties of Transition Metal Compounds: Introduction to the Theory. Wiley-Interscience, New York.

Dereń, P.J., Stręk, W., Oetliker, U. and Güdel, H.U. (1994) Spectroscopic properties of Co^{2+} ions in $MgAl_2O_4$ spinels. Physica status solidi (b), 182, 241-251.

Feenstra, A., Ockenga, E., Rhede, D. and Wiedenbeck, M. (2003) Li-rich zincostaurolite and its decompression-related breakdown products in a diaspore-bearing metabauxite from East Samos (Greece): An EMP and SIMS study. American Mineralogist, 88, 789-805.

Ferguson, J. (1963) Crystal-field spectra of $d^{3,7}$ ions. I. Electronic absorption spectrum of $CoCl_4^-$ in three crystalline environments. The Journal of Chemical Physics, 39, 116-128.

Ferguson, J., Wood, D.L. and Van Uitert, L.G. (1969) Crystal field spectra of $d^{3,7}$ ions. Tetrahedral Co^{2+} ion in $ZnAl_2O_4$ spinel. The Journal of Chemical Physics, 51, 2904-2910.

Gruen, D.M. and McBeth, R.L. (1963) Coordination chemistry of 3*d* transition metal ions in fused salt solutions. Pure and Applied Chemistry, 6, 23–47.

Hochu, F. and Lenglet, M. (1998) Co(II) optical absorption in spinels: infrared and ligand-field spectroscopic study of the ionicity of the bond. Magnetic structure and $Co^{2+} \rightarrow Fe^{3+}$ MMCT in ferrites. Correlation with the magneto-optical properties. Active and Passive Electronic Components, 20, 169-187.

Keppler, H. (1992) Crystal field spectra and geochemistry of transition metal ions in silicate melts and glasses. American Mineralogist, 77, 62-75.

Koch-Müller, M. (1997) Staurolithe im System $MgO\text{-}FeO\text{-}Al_2O_3\text{-}SiO_2\text{-}H_2O$: Synthese, Charakterisierung, Thermodynamik. Habilitationsschrift, TU Berlin, Germany, 220 p.

Kuindersma, S.R., Boudewijn, P.R. and Haas, C. (1981) Near-infrared d-d transitions of NiJ_2, CdI_2:Ni^{2+}, and CoI_2. Physica status solidi (b), 108, 187-194.

Levy, D., Pavese, A., Sanni, A. and Rischedda, V. (2001) Structure and compressibility of synthetic $ZnAl_2O_4$ (gahnite) under high-pressure conditions, from synchrotron X-ray powder diffraction. Physics and Chemistry of Minerals, 28, 612-618.

Marfunin, A.S. (1979) Physics of minerals and inorganic materials: an introduction. Springer-Verlag, New York.

Nasu, T. (1975) Optical absorption spectra of Co^{2+} ion in KC1 and NaCl crystals. Physica status solidi (b), 70, 97-105.

Phillips, L.V. and Griffen, D.T. (1986) Staurolite-lusakite series. I. Synthetic Fe-Co staurolite. American Mineralogist, 71, 1461-1465.

Peterson, R.C., Lager, G.A, and Hitterman, R.L. (1991) A time-of-flight neutron powder diffraction study of $MgAl_2O_4$ at temperatures up to 1273 K. American Mineralogist, 76, 1455-1458.

Rossman GR, Taran MN (2001) Spectroscopic standards for four- and five-coordinated Fe^{2+} in oxygen-based minerals. American Mineralogist 86, 896-903.

Skogby, H. and Hålenius, U. (2003) An FTIR study of tetrahedrally coordinated ferrous iron in the spinel-hercynite solid solution. American Mineralogist, 88, 489–492.

Skerl, A.C., Bannister, F.A. and Groves, A.W. (1934**)** Lusakite, a cobalt-bearing silicate from Northern Rhodesia. Mineralogical Magazine, 23, 598-606.

Taran, M.N. and Koch-Müller, M. (2009) Optical spectroscopic study of natural Fe-rich Pizzo Forno staurolite at different temperatures and pressures. American Mineralogist (submitted).

Taran, M.N., Koch-Mueller, M., Langer, K. (2005) Electronic absorption spectroscopy of natural (Fe^{2+}, Fe^{3+})-bearing spinels of spinel s.s.-hercynite and gahnite-hercynite solid solutions at different temperatures and high-pressures. Physics and Chemistry of Minerals, 32, 175-188.

Taran, M.N. and Langer, K. (2001) Electronic absorption spectra of Fe^{2+} ions in oxygen-based rock-forming minerals at temperatures between 297 and 600 K. Physics and Chemistry of Minerals, 28, 199-210.

Taran, M.N., Langer, K. and Geiger C.A. (2002) Single-crystal electronic absorption spectroscopy of synthetic chromium-, cobalt-, and vanadium-bearing pyropes at different temperatures and pressures. Physics and Chemistry of Minerals, 29, 362-368.

Taran, M.N., Ohashi, H. and Koch-Müller, M. (2008) Optical spectroscopic study of synthetic $NaScSi_2O_6$–$CaNiSi_2O_6$ pyroxenes at normal and high pressures. Physics and Chemistry of Minerals, 35, 117-127.

Yamanaka T, Takéuchi Y (1983) Ordering-disordering transition in $MgAl_2O_4$ spinel at high temperature up to 1700 °C. Zeitschrift für Kristallographie, 165, 65-78.

Captions for Figures

Figure 1. Optical absorption spectrum of natural Co-bearing spinel at ambient conditions.

Figure 2. Polarized optical absorption spectra of natural Co-bearing staurolite at ambient conditions.

Figure 3. Optical absorption spectra of Co-bearing spinel measured at different temperatures.

Figure 4. Polarized optical absorption spectra of Co-bearing staurolite at room temperature (24 °C) and 300 °C.

Figure 5. Optical absorption spectra of Co-bearing spinel at different pressures.

Figure 6. Unpolarized optical absorption spectra of Co-bearing staurolite at different pressures.

Table 1. Results of EMPA and SIMS (Li) of the two samples of Co-bearing staurolite (**ac**- and **ab**-sections) in atoms pfu calculated on the basis of 46 oxygens and assuming total iron as ferrous. The data are averaged over 22 and 11 measurements, respectively, (1 σ standard deviation).

	Si	Ti	Al	Cr	V	Fe	Mg	Mn	Zn	Ni	Co	Li
ac	8.087(96)	0.037(7)	17.593(103)	0.008(4)	0	0.831(27)	0.089(5)	0.034(4)	1.648(68)	0.203(50)	0.175(11)	0.740(5)
ab	8.214(38)	0.012(6)	17.749(44)	0.029(15)	0	0.587(22)	0.117(7)	0.032(5)	1.593(33)	0.069(8)	0.109(12)	0.745(4)

Table 2. Energy, in cm^{-1}, of the main absorption bands of $^{IV}Co^{2+}$ in spectra of natural spinel (Fig. 1) and staurolite (Fig. 2) at ambient conditions.

	Spinel band	Staurolite band
a	6640	5350
b	7070	5750
c	7730	6230
d	16080	7380
e	16840	8250
f	18260	15650
g	20920	17240
h		18830

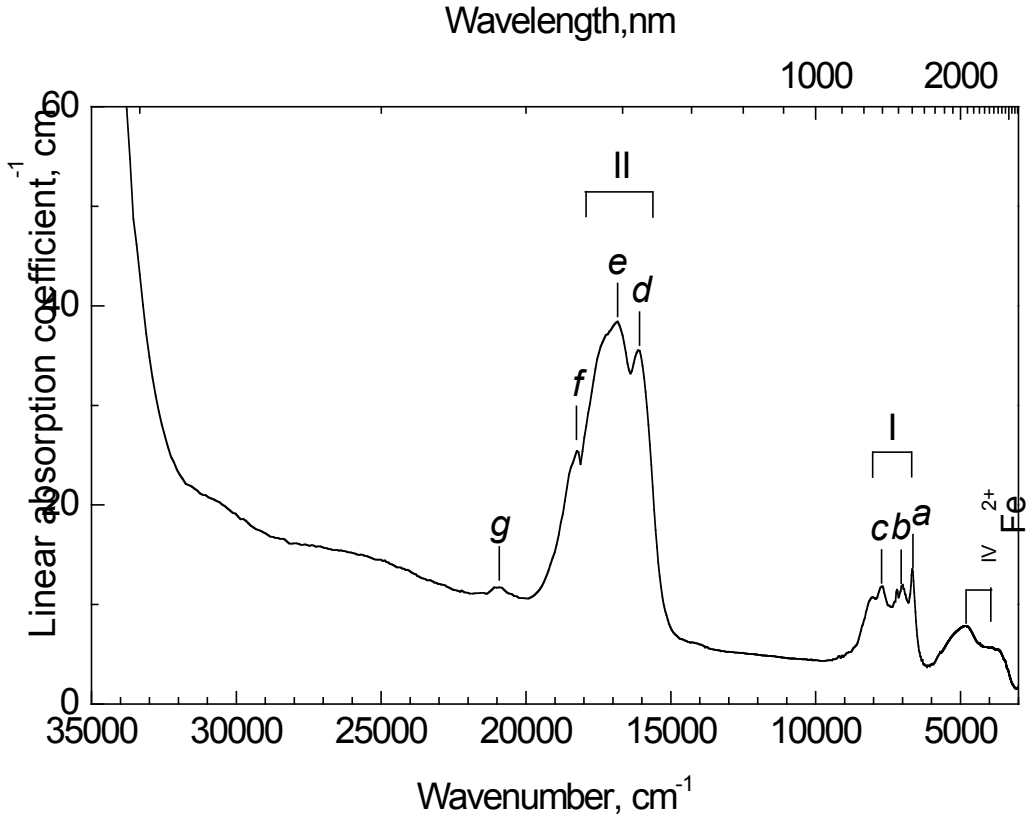

Figure 1. Optical absorption spectrum of natural Co-bearing spinel at ambient conditions.

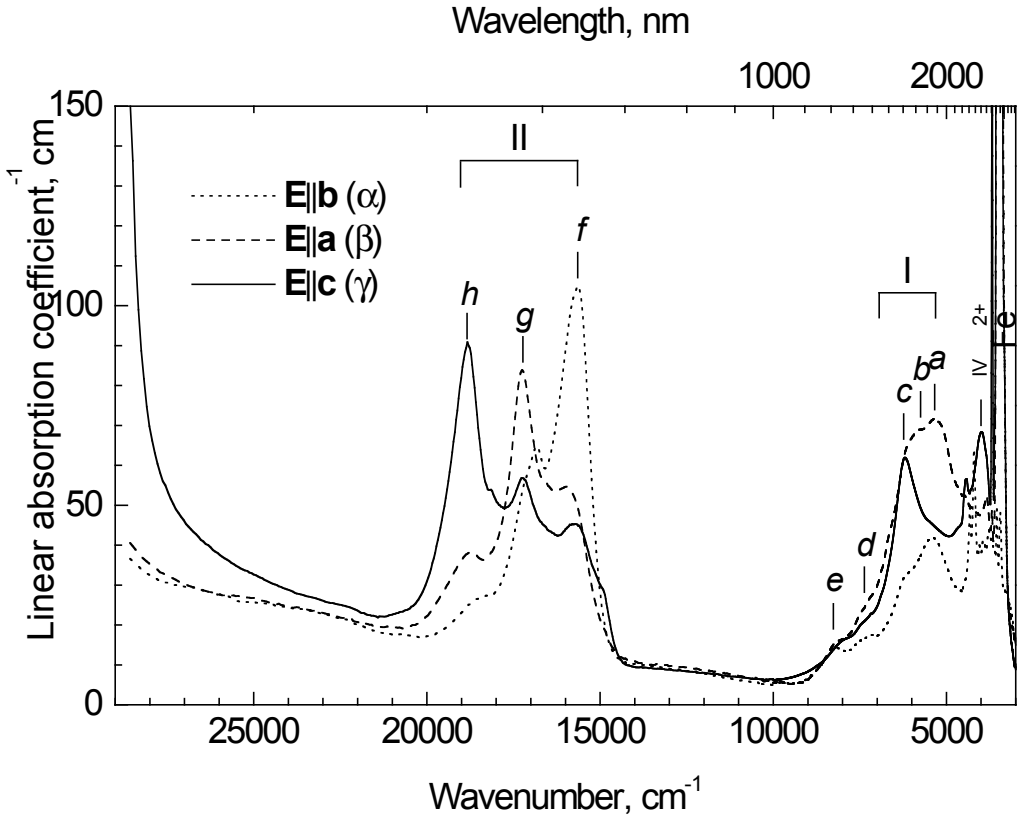

Figure 2. Polarized optical absorption spectra of natural Co-bearing staurolite at ambient conditions.

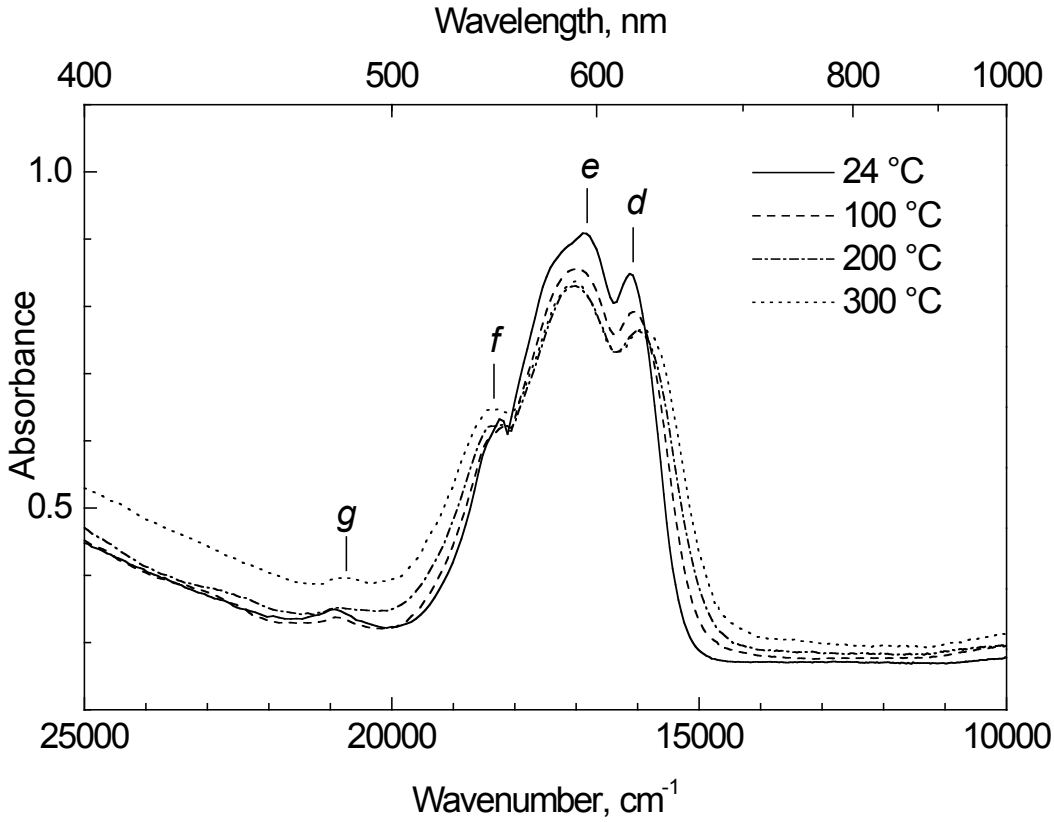

Figure 3. Optical absorption spectra of Co-bearing spinel measured at different temperatures.

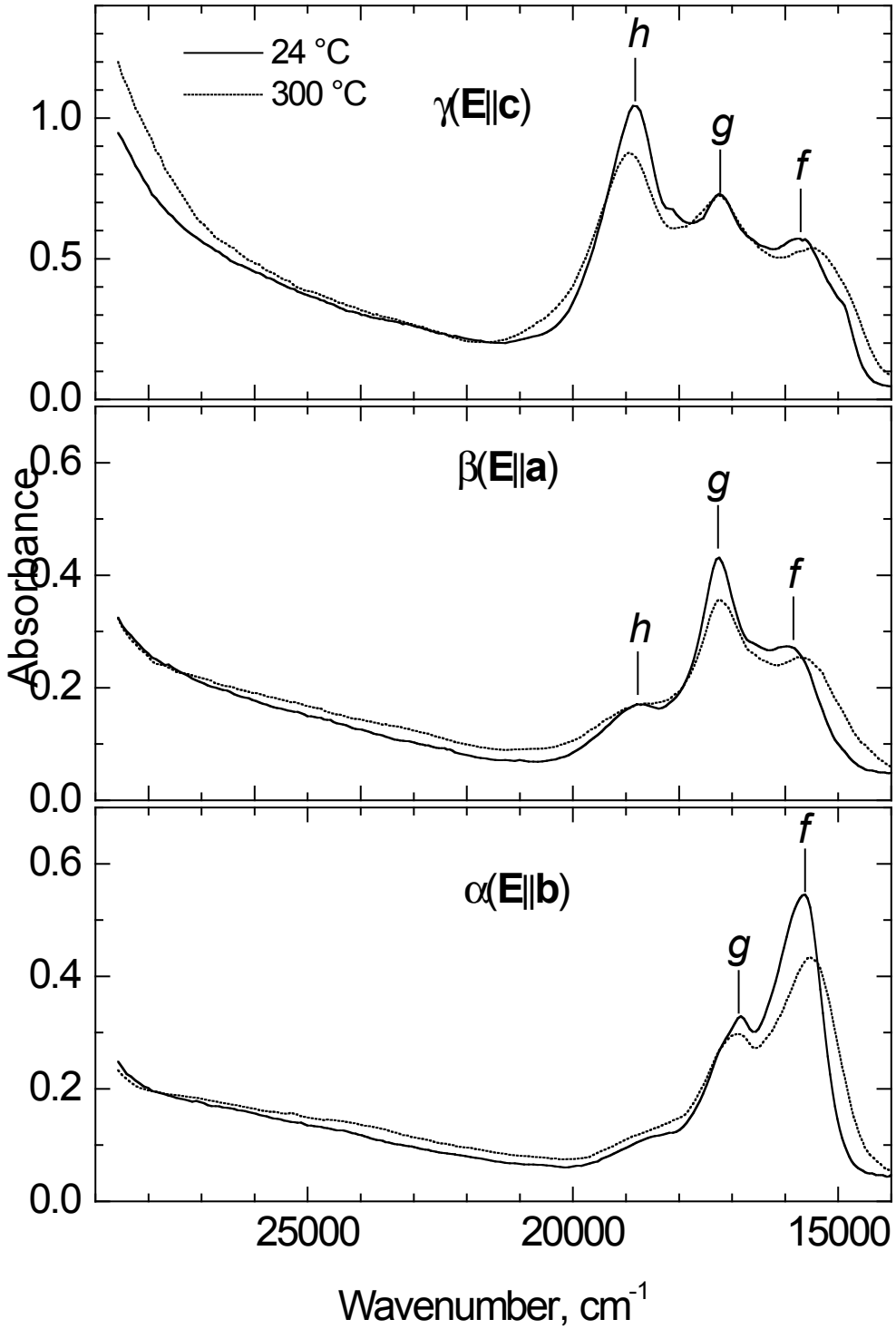

Figure 4. Polarized optical absorption spectra of Co-bearing staurolite at room temperature (24 °C) and 300 °C.

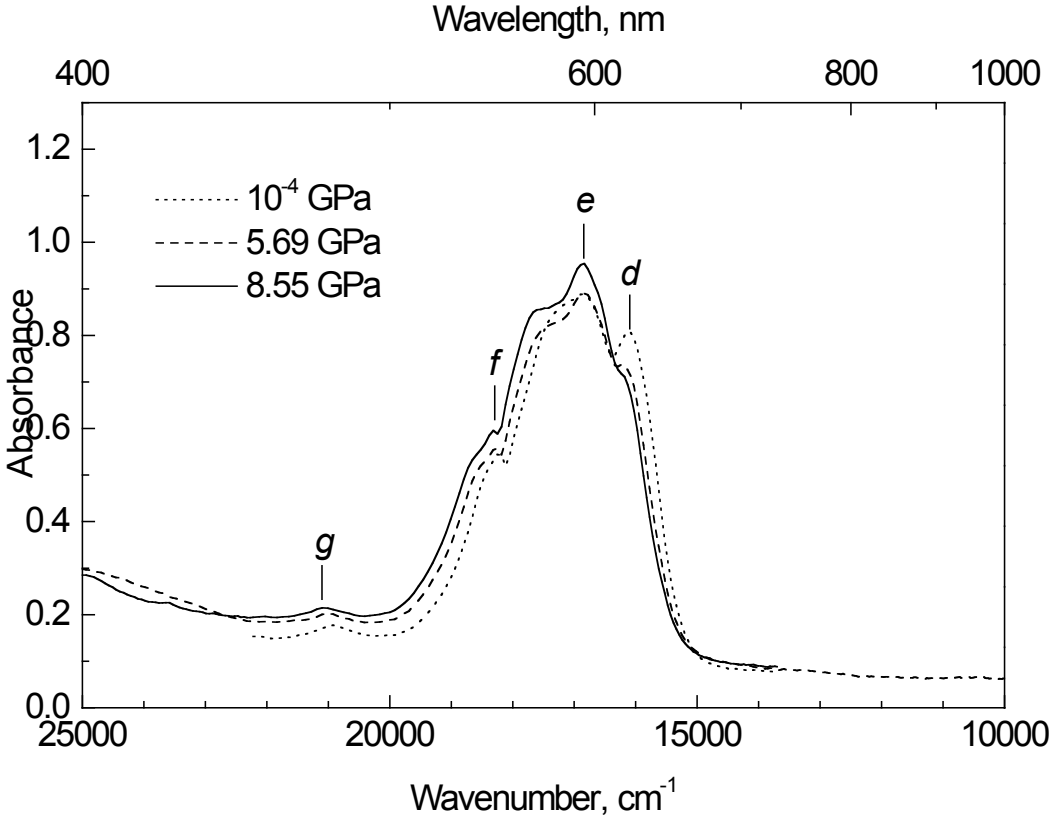

Figure 5. Optical absorption spectra of Co-bearing spinel at different pressures.

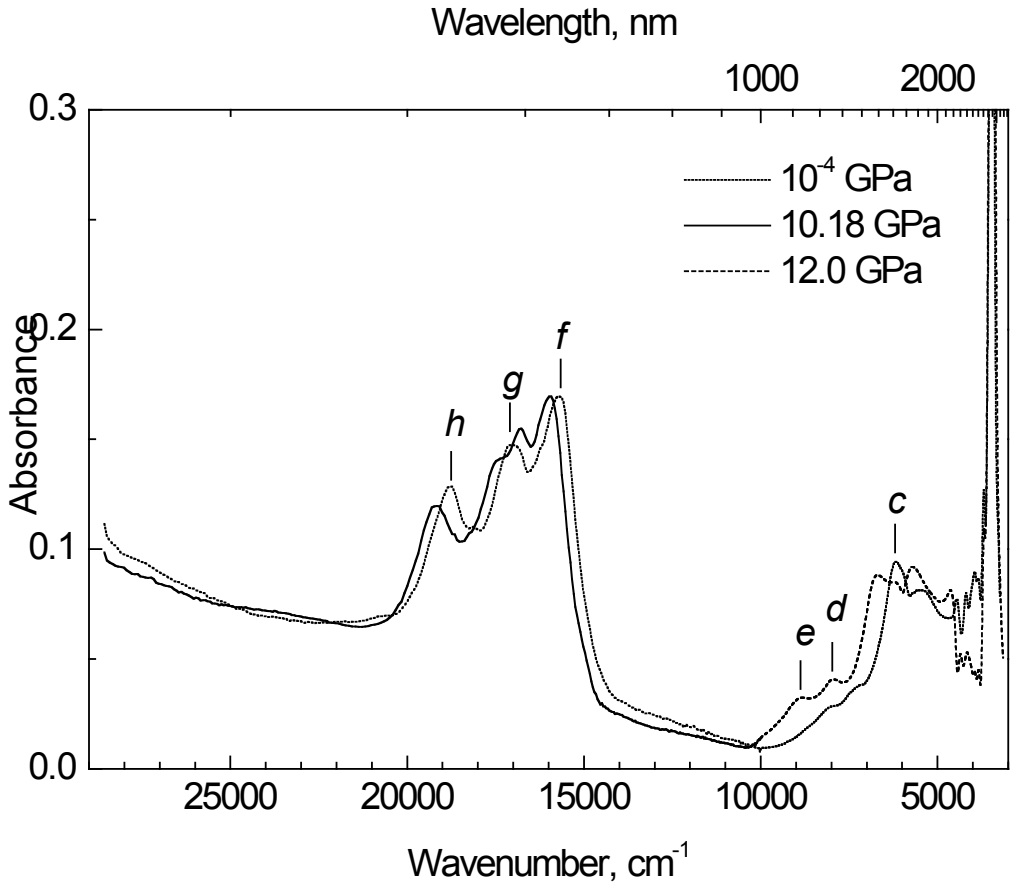

Figure 6. Unpolarized optical absorption spectra of Co-bearing staurolite at different pressures.